A 3-level Model for Schumann-Runge O_2 Laser-Induced Fluorescence

Glenn S. Diskin*
NASA Langley Research Center
Hampton, Virginia

Walter R. Lempert† and Richard B. Miles‡
Princeton University
Princeton, New Jersey

Abstract

A three level model has been developed for the analysis of Schumann-Runge band ($B^3\Sigma_u^- \leftarrow X^3\Sigma_g^-$) laser-induced fluorescence of molecular oxygen, O_2. Such a model is required due to the severe lower state depletion which can occur when transitions having relatively large absorption cross-sections are excited. Such transitions are often utilized via ArF* or KrF* excimer or dye-laser excitation in high temperature environments. The rapid predissociation of the upper state prevents substantial repopulation of the lower state by collisional processes, and the lower state may be largely depleted, even at laser fluences as low as 10-100 mJ/cm^2. The resulting LIF signal in such cases no longer varies linearly with laser pulse energy, and the extent of the sublinear behavior varies with the particular rovibrational transition of interest. Relating the measured signal to the lower state population, then, necessitates the use of exceedingly low laser fluences. These low fluences in turn lead to the need to compromise spatial resolution in order to generate sufficient signal.

Introduction

The Schumann-Runge (S-R) band system ($B^3\Sigma_u^- \leftarrow X^3\Sigma_g^-$) of molecular oxygen, O_2, has been the subject of much study, due primarily to its importance in atmospheric photochemistry. Measurement of flow properties by use of S-R laser-induced fluorescence (LIF), has grown in scope since Massey and Lemon[1] first proposed the use of a tunable ArF* laser for the measurement of temperature and density in air. Since that time, S-R LIF has been used to measure single-point temperature and density in low-temperature flows using an ArF* laser,[2] for imaging and detection of hot O_2 in combustion systems using ArF*, KrF* and dye laser systems,[3-7] and for measurement of temperature in high temperature air using a KrF* laser.[8] S-R LIF has also been used in conjunction with stimulated Raman scattering to perform velocity measurements in air flows.[9] S-R band LIF is often used because (1) oxygen is naturally present in many flow situations, and therefore doesn't need to be seeded into the flow, and (2) the upper, or *B*-state in the S-R band system is rapidly predissociated, eliminating the need for quenching corrections and providing a signal which is directly proportional to lower state number density. An unfortunate consequence of the rapid predissociation of the upper state is that the quantum yield, or fluorescence efficiency, of the fluorescence emission is very low, typically on the order of 10^{-4}. Additionally, numerous authors have reported sublinear signal generation at moderate laser fluences,[4,6,8] due primarily to lower state depletion, or bleaching. The purpose of this paper is to describe a model constructed to simulate the O_2 S-R LIF signal generation process.

Analysis of the signal obtained in a laser-induced fluorescence experiment requires a means to relate the measured signal to the population in the state of interest, i.e. the lower state involved in the excitation transition. In order to relate the collected signal to the lower state population, one must construct an appropriate model. This model should include the processes of laser excitation and de-excitation to and from the upper state of the transition, de-excitation of the upper state by radiative decay (fluorescence), predissociation and collisional quenching, and redistribution of lower and upper state populations by collision-induced energy transfer (rotational and/or vibrational). The large predissociation rates associated with transitions in the O_2 Schumann-Runge sys-

---

* Research Engineer, Hypersonic Airbreathing Propulsion Branch, Member AIAA.

† Research Scientist, Department of Mechanical and Aerospace Engineering, Member AIAA.

‡ Professor, Department of Mechanical and Aerospace Engineering, Senior Member AIAA.

tem render a simple steady-state, two-level model, such as described by Eckbreth[10], inappropriate. A model more appropriate for O_2 Schumann-Runge laser-induced fluorescence was described by Laufer, et al.[2] This quasi-two-level model includes the relevant processes, and uses an analytical integration of the rate equations (for top-hat temporal laser excitation) to relate the signal to the lower state population. The model works well for predissociation-dominated transitions with laser intensities low enough not to encounter significant population depletion. Transitions in O_2 from the ground vibrational level excited by an ArF* laser (the (4,0) band) fall into this category.

The model described in Ref. [2] does not adequately account for depletion of the lower vibrational manifold when the laser excitation becomes large and collisional rotational repopulation rates become large. The reason for this is that the lower ro-vibrational level was assumed in Ref. [2] to have an infinitely large bath from which collisional repopulation can occur. It is more realistic to assume that this lower level can only be refilled by those molecules which began the process in the same vibrational level, i.e. that vibrational re-equilibration times are much greater than typical laser pulse times and that rotational re-equilibration times are comparable to laser pulse times. To keep track of this depletable bath, a new model was constructed which extends the model of Ref. [2] in two ways. First, a third level was included. This level represents all of the rotational levels of the ground vibrational level except the one coupled to the upper state by the laser, and provides the bath of molecules from which the lower level may be refilled. Second, since for transitions stronger than the (4,0) band the absorption rate may be comparable to the predissociation rate, the process of stimulated emission must be included as a mechanism to couple the upper and lower states. The stimulated emission terms, which were dropped in the simplification of Ref. [2], are retained in this model.

Inclusion of a third level in the model takes away the elegance of the solution given in Ref. [2], in that the solution can no longer be represented in terms of a simple function of two parameters. The analytical solution becomes a very messy algebraic expression which doesn't allow for easy assessment of the effects of individual parameters. The system of equations was therefore solved numerically. This solution method has the advantage that a more realistic laser pulse shape can be employed; Laufer, et al.[2] solved the quasi-two-level problem for a top-hat excitation pulse shape. For the solutions described herein, a Gaussian temporal distribution was used. A benefit of calculating the temporal response of the system using a realistic excitation temporal profile is an improvement in the representation of nonlinear effects. This is due to the fact that the system responds differently to excitation of high and low intensity; a 'real' temporal pulse shape incorporates a distribution of intensities, while a top-hat pulse lumps everything into a single, uniform value. What precisely is meant by 'high' and 'low' intensity is, of course, determined by the particular system.

Three-level LIF Model

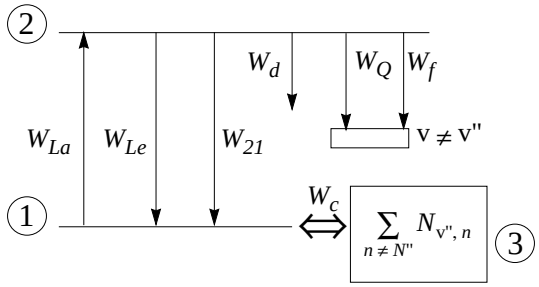

Using the notation of Ref. [2], the equations governing the three-level system are:

$$\frac{dN_1}{dt} = -W_{La}(t) \cdot N_1 + N_2 \cdot (W_{Le}(t) + W_{21}) + W_C \cdot \left(\frac{f_B}{1 - f_B} \cdot N_3 - N_1 \right) \quad (1)$$

$$\frac{dN_2}{dt} = W_{La}(t) \cdot N_1 - N_2 \cdot (W_{Le}(t) + W_d + W_{21} + W_f + W_Q) \quad (2)$$

$$\frac{dN_3}{dt} = -W_C \cdot \left(\frac{f_B}{1 - f_B} \cdot N_3 - N_1 \right) \quad (3)$$

In this model, described by equations (1)-(3) and depicted schematically above, levels 1 and 2 represent the ro-vibrational levels in the ground and excited electronic states, respectively, which are coupled by the laser frequency. Level 3 consists of the bath of molecules collisionally coupled to level 1, by the rate W_c. The factor $f_B/(1\text{-}f_B)$ which precedes the N_3 term in equations (1) and (3) is required to provide detailed balancing of the forward and reverse collisional redistribution processes. The model includes the relevant processes of laser-stimulated absorption and emission (W_{La} and W_{Le}), spontaneous emission (W_{21}), predissociation (W_d), collisional quenching of the upper state (W_Q), and radiative decay to vibrational levels other than the lower level of the transition (the fluorescence of interest, W_f).

Not included in this model is collisional redistribution of rotational or vibrational energy in the upper level, as these are considered to be slow with respect to the predissociation.

The primary parameter of interest for the user of this model is the fluorescence signal, denoted S_f. The fluorescence signal at any time, *t*, per unit volume, emitted into 4π steradians, $\hat{S}_f(t)$, is equal to $W_f^* \cdot N_2(t)$, and the total signal generated during the laser pulse is:

$$\hat{S}_f = \int_{t_p} W_f^* \cdot N_2(t) dt , \qquad (4)$$

where t_p is the laser pulse duration and W_f^* is the portion of the fluorescence signal which is detectable due to spectral filtering. In order to obtain the quantity $\hat{S}_f$, equations (1)-(3) must be integrated to find $N_2(t)$, which is then integrated according to equation (4). To perform the required integration, appropriate values for the parameters W_c, W_d, W_f, W_{21} and f_B must be found, as well as an appropriate functional form of $W_L(t)$. With these values, discussed subsequently, equations (1)-(4) can be integrated numerically using one of the standard techniques. For this work, the public domain software package Octave [11], version 1.1.1, was employed. Octave provides a front-end for the Lawrence Livermore ordinary differential equation solver, LSODE [12], written by Alan C. Hindmarsh.

Parameters in the Rate Equations

In order to solve the equations governing the model system, the parameters W_c, W_d, W_Q, W_f, W_{21} and f_B must be found. W_c is the collisional repopulation rate in the lower vibronic level (N_1), and is a function of the fluid density and temperature. W_d is the upper rovibronic predissociation rate, and is only a function of the upper level quantum state, as are W_f, the fluorescence rate, and W_{21}, the rate of spontaneous emission at the laser frequency. W_Q is the collisional quenching rate, and is a function, in general, of the temperature and densities of all collision partners. The rotational Boltzmann fraction associated with the lower level, f_B, is a function of temperature, the lower vibrational level, and the lower rotational level. The laser excitation rate parameters, $W_{La}(t)$ and $W_{Le}(t)$, should be decomposed into their various pieces so that they can be better understood. As described in Ref. [10],

$$W_{La}(t) = I_L(t) \cdot \mathrm{B}_{12} \cdot \varphi / \mathrm{c} \qquad (5)$$

$$W_{Le}(t) = I_L(t) \cdot \mathrm{B}_{21} \cdot \varphi / \mathrm{c} \qquad (6)$$

where $I_L(t)$ is the time-dependent laser intensity, B_{12} and B_{21} are the Einstein coefficients for absorption and emission, respectively, and φ is the overlap integral of the transition and laser lineshapes.

$$\varphi = \int_{\Delta\bar{\nu}} g(\bar{\nu}) h(\bar{\nu}) d\bar{\nu} ,$$

where $\int_{\Delta\bar{\nu}} g(\bar{\nu}) d\bar{\nu} = 1$ and $\int_{\Delta\bar{\nu}} h(\bar{\nu}) d\bar{\nu} = 1$

and $g(\bar{\nu})$ and $h(\bar{\nu})$ are the transition and laser lineshapes, respectively. The symbol $\bar{\nu}$ is defined as ν / c.

The Einstein coefficient B_{12} used in equation (5) applies to the ro-vibrational transition of interest, and is given by

$$B_{12} = \frac{A_{21}}{8\pi h c \bar{\nu}^3} \cdot \frac{S^R{}_J}{2J'' + 1} \cdot \frac{g_u}{g_l} ,$$

where $S^R{}_J$ is the rotational line strength and is given in Ref. [13] for each of the branches of ${}^3\Sigma$-${}^3\Sigma$ transitions. The coefficient B_{21} is given as $B_{12} \cdot g_l/g_u$. The A_{ij} used for the calculations presented herein were taken from Ref. [14]; W_{21} and W_f are found from the same A_{ij} data.

The remaining component of $W_L(t)$ is $I_L(t)$. The temporal pulse shape of the ArF* excimer laser used in this work can be closely approximated by a Gaussian distribution with a 15 ns FWHM (τ); the KrF* of Ref. [8] by a Gaussian with τ=20 ns. Noting that the laser pulse energy, E_L, is equal to the integral of the product of the beam area, *A*, and its intensity, the laser temporal intensity is given by,

$$I_L(t) = \frac{\Phi}{\tau} \cdot \sqrt{\frac{4\ln 2}{\pi}} \cdot e^{-4\ln 2 \cdot \left(\frac{t - t_0}{\tau}\right)^2} , \qquad (7)$$

where $\Phi = E_L/A$ is the laser fluence.

The predissociation rates were taken from references [15] and [16], converting from linewidths (FWHM) by $W_d = 2\pi c \cdot \Delta\bar{\nu}_{\mathrm{pre}}$.

The electronic quenching rate for the *B*-state of O_2 is not known, due to the fact that it typically competes poorly with that state's rapid predissociation. For upper vibrational levels v'=0 and v' > 12, though, the quenching rate *may* be comparable to the low predissociation rates of those levels. Based on data provided in Ref. [6], in which no effects of quenching were seen in an atmospheric pressure flame for v'=0, N'=18, we assume a maximum quenching rate at those conditions of 1/10 of that state's predissociation rate. Also assuming no variation in quenching cross-section with temperature, we have: $W_Q = 7.8 \cdot 10^9 \ \mathrm{p} \cdot (300/\mathrm{T})^{1/2} \ \mathrm{sec}^{-1}$. This rate is com-

parable to quenching rates for other electronically excited species. This rate is comparable at atmospheric pressure to the predissociation rates for v'=0 and v' > 12, and therefore must be included in the model.

Estimation of the collisional refilling rate, W_c

The final parameter required is the collisional redistribution rate, W_c. That this is written as a singular parameter represents a great simplification in the dynamic rotational energy transfer processes which occur in the probed medium during the period of laser-induced removal of molecules from a single rotational level, or even sublevel. A more complete model would include the summation of a number of rotational energy transfer reactions of the form,

$$N_{i,v} + N_{j-1,v} \Leftrightarrow N_{i-1,v} + N_{j,v} \tag{8}$$

with appropriate forward and reverse rate coefficients. Similar expressions could be written for reactions involving the transfer of multiple rotational quanta. The result would be a set of ordinary differential equations, one for each of the rotational levels in each of the vibrational levels, possibly including each of the electronic levels, for all of the chemical species present. Clearly, the complete model would be algebraically cumbersome and would necessitate evaluation of each of the transfer rates. If one compares the expressions derived from equations of the form of equation (8) to equation (3), one may interpret the rate W_c as the product of the population of the local bath of molecules and a Boltzmann fraction-weighted rotational transfer rate. This interpretation of the collisional repopulation rate causes difficulty in assigning a value to it for the purpose of using the model. A simpler interpretation and assessment of the rate, W_c, follows.

Whenever a molecule in a level 1 is removed by absorption of a photon, the equilibrium of the rovibrational distribution is disturbed. The restoration of the local equilibrium occurs through the effects of collisional redistribution of energy among the remaining molecules. This redistribution process, then, is in some way related to the bimolecular collision rate. The collisions which are expected to be important are those involving molecules in the energetic neighborhood of level 1, and an unspecified partner. In order for collisions to be effective in the context of this model, their effect must be felt in the time-frame of the laser pulse. Due to the relative slowness (with respect to the laser pulse length, τ) of vibrational re-equilibration, only the vibrational level containing level 1 will be considered to contribute to the replenishment of level 1, for the purpose of this model.

For O_2 S-R LIF, the upper and lower electronic states are both triplet states. Due to the coupling of the molecule's nuclear angular momentum and electron spin angular momentum, the energies of the three spin components of each level are slightly different. That these differences are not identical in the upper and lower rovibronic levels is the source of observable triplet splitting. As is customary, we denote N the quantum number for angular momentum excluding electron spin, and J the quantum number including spin. For each N, the possible J values are N-1, N, and N+1. Although the spin components are usually unresolved or only partially resolved in absorption, this is not always the case. For the cases where only one or two components may be excited, we need to take into account any collisional coupling between molecules of differing electron spin. The microwave absorption data provided in Ref. [17] include half-linewidths for (N", J") levels for v"=0. These lifetimes are related to the collisional rates by $W_c = 2\pi c \cdot \Delta\bar{\nu}_{\mu wave}$. Ref [17] also provides information about the spin re-equilibration, by invoking a *propensity rule*. By this rule, collisions which change electron spin are unlikely, due to the weak coupling in O_2 between the electron spin angular momentum and the nuclear angular momentum.

Using this information, the bath of molecules which may collisionally replace those molecules removed from the lower state of the transition consists, for the purpose of this model, of those molecules in the same vibrational level and having the same electron spin as those of the lower state of the transition. In other words, each electron spin group acts as if it is independent of the others, and its bath consists of the molecules of like spin in the remaining rotational levels in the lower vibronic state.

Using an average value of the half-widths from Ref. [17], and assuming that the collision cross-section is independent of temperature, we estimate $W_c = 7.78 \cdot 10^9 \, p \cdot (300/T)^{1/2} \, sec^{-1}$.

With the understanding of level 3 as the bath described above, it is clear that the Boltzmann fraction, f_B, used in equations (1) and (3) is the *rotational* portion of the complete Boltzmann fraction in the lower vibronic state, and must be computed for the initial rotational temperature of the gas.

$$f_B = \frac{2J'' + 1}{Q_r} \cdot e^{-F_{v''}(N'', J'') \cdot hc/kT}, \tag{9}$$

where Q_r is the rotational partition function and $F_{v''}(N'',J'')$ is the rotational energy associated with v'', N'' and J''.

One final comment is in order, regarding the use of the microwave-derived collisional transfer rate. The microwave absorption is a purely spin-changing process, i.e. the nuclear angular momentum is unchanged. For this reason, the disturbance to rotational equilibrium associated with the absorption of microwave radiation is expected to be small. Under intense excitation, however, Schumann-Runge electronic absorption may significantly perturb the local rotational energy distribution, removing molecules preferentially from the energetic neighborhood of level 1. The relationship between the microwave linewidths and the rotational refilling rate, W_c, under such conditions may no longer be valid.

Calculations using the Model

Calculations were made of the laser-induced fluorescence signal, $\hat{S}_f$, as a function of the laser fluence, Φ, for relevant rotational states in several of the vibrational bands accessible using the ArF* or KrF* excimer lasers. Prior to integration, variables were normalized by appropriate constants, as follows:

$$\hat{N}_1 = N_1/N_{1,0},\ \hat{N}_2 = N_2/N_{1,0},$$

$$\hat{N}_3 = N_3/N_{3,0} = (N_3/N_{1,0}) \cdot f_B/(1 - f_B).$$

For each set of parameter values, equations (1) - (4) were integrated forward in time from the initial conditions, $\{t_0 = 0.,\ \hat{N}_1 = 1.,\ \hat{N}_2 = 0.,\ \hat{N}_3 = 1.\}$, past the completion of the laser pulse, until the fluorescence signal had reached its final value. A representative plot of the time histories, for the (15,3) $R_1(11)$transition, using f_B=0.127, Φ=25 mJ/cm^2 is shown in Figure 1. The value of f_B is consistent with a rotational temperature of approximately 300K. In the Figure, the strong laser excitation causes N_1 to drop rapidly, while the large value of W_c at atmospheric pressure and room temperature causes N_3 to follow closely behind N_1. This relatively rapid refilling allows significantly more signal to be generated than would have been in the absence of collisional refilling. The strong excitation nevertheless causes a reduction in the lower state population available for pumping, and hence a reduction in signal from that which would have been generated if N_1 were able to remain essentially constant. Near the peak of the laser pulse, N_2 is approximately 2% of N_1, and hence stimulated emission does not cause a significant reduction in signal in this case. The resultant signal is only 44% of that which would be achieved with infinitely fast refilling from an inexhaustible bath, i.e. N_1=$N_{1,0}$=constant. As the pulse finishes, rotational re-equilibration between N_1 and N_3 occurs, and the final lower state population is only ≈0.17 of its initial value. Hence, approximately 83% of the initial population in the lower vibronic state has been lost, to predissociation and via both radiative and nonradiative decay to other vibrational levels in the lower electronic state. The majority of this loss is to predissociation, for the conditions described.

Comparisons with Data

In order to assess the performance of the model, a comparison was made between calculations such as these and experimental laser-induced fluorescence data. A sequence of calculations was performed for each of several transitions, for a range of laser fluence, Φ, from $10^{-1}$to 10^{+3} mJ/cm^2. Two sets of experimental data were used for comparison. The first set was obtained from Ref. [8], which contains data for air at 1800K, for the (2,7) P(9) and (0,6) R(17) transitions excited by an injection-locked KrF* excimer laser. The bandwidth and pulse duration of this laser were reported to be 0.8 cm^{-1} and 20 ns, respectively. Comparisons of these data with model calculations are shown in Figures 2(a) and(b). The agreement is seen to be excellent for the (2,7) transition, and although the model somewhat overpredicts the depletion observed for the (0,6) excitation, the agreement is still good enough to provide a reasonable assessment of the fluence at which nonlinear behavior becomes a concern.

The second data set was obtained in a manner identical to that described in Ref.[18], in a variation of the RELIEF technique. These data were collected by conducting an excitation scan for each of three nominal values of ArF* laser pulse energy, after preparing prior to each laser pulse a sample of vibrationally excited O_2 by stimulated Raman scattering (SRS) and allowing the vibrational distribution to evolve for a fixed period of time (1.0 μs). During this time interval, vibrational-to-vibration energy transfer creates a substantial population in v">1, while leaving the rotational temperature substantially unchanged. These vibrationally excited states may be probed using S-R LIF. The variation in ArF* laser fluence was achieved by inserting zero, one or two thicknesses of an absorbing glass into the beam path. The glass chosen absorbed approximately 30% of the light, and so the pulse energy was varied by an order of magnitude over this sequence of excitation scans. For each excitation scan, the ArF* laser wavelength was incremented by 1 step (equivalent to 0.0493 cm^{-1}) for each data point, and the scan encompassed 700 grating steps. Due to absorption of the laser beam by atmospheric O_2, the energy arriving at the measurement location varied over the course of the excitation scan; a PIN photodiode provided a monitor for the energy arriving at the measurement location. The LIF data from the excita-

tion scans were least-squares fit to a sum of Voight profiles, and the transition-specific peak values were extracted. The data from these three excitation scans thus consisted of three line-center signals for each of the transitions excited in the scan, each at a different ArF* laser fluence. Due to the congested nature of the S-R spectrum and the broadband spectral signal collection, only one unambiguous transition could be isolated, namely the (15,3) $R_1(11)$ line. The range of laser fluence utilized in this test was not sufficient to provide data in the linear (non-depleting) regime, but the lowest fluence is predicted by the model to be within 10% of linear. A plot of line-center signal versus laser fluence for the (15,3) $R_1(11)$ transition at a rotational temperature of 300K is shown in Figure 3. The experimental data and model calculation have been forced to the same value at a fluence of 6 mJ/cm^2, and the model reasonably predicts the signal levels for the higher fluences. It should be pointed out that the *vibrational* temperature associated with these data is undefined, as the vibrational energy distribution is evolving in time following the SRS event.

Imaging of S-R LIF

The results presented in Figures 2 and 3 provide justification for using this 3-level model in a predictive mode. In the course of designing a LIF experiment, one must estimate signal levels, in order to determine the spatial resolution achievable for a particular laser fluence, at some nominal thermodynamic conditions. The data presented have shown that simply increasing the laser fluence in order to increase signal is not an option when using O_2 S-R LIF. At relatively low fluences, the signal no longer varies linearly with laser fluence; one must therefore operate below this level. It is not possible to operate in a fully saturated regime, since in the limit of very large laser fluence and complete depletion of N_1, the signal is still dependent on the collisional refilling rate. This rate, as discussed earlier, is a function of the local thermodynamic conditions, and the signal obtained, then, would also be a function of those conditions.

The quantity that is needed, in order to design an LIF experiment, then, is the maximum laser fluence one may use, while remaining nominally in the linear regime. Operation in the linear regime allows the lower state population to be deduced from the signal without needing to understand the temporal dynamics of the signal generation process. Operation in this regime also allows correction of signal variations which are due to laser energy fluctiuations. If the departure from linear behavior is limited to, say, 5%, the maximum laser fluence allowable can be predicted for any transition, using this 3-level model. With this maximum fluence and appropriate signal collection and detection efficiencies, the maximum measurable linear signal can be calculated. The equation for signal photons collected per pixel, as derived in Ref. [10], is

$$NPP_{max} = \Phi_{max} \cdot V\eta_{coll} \cdot n \cdot \frac{B_{12} \cdot \varphi}{c} \cdot \eta_f , \qquad (10)$$

where η_f is the fluorescence efficiency, or Stern-Volmer factor, V is the fluid volume element and η_{coll} is the combined collection / detection efficiency. The quantity n is the number density of molecules in level 1; $n=N_T X_{O2} \alpha_{v"} f_B \kappa / g_{elec}$, where $N_T X_{O2}$ is the O_2 number density, $\alpha_{v"}$ is the *vibrational* Boltzmann fraction and κ / g_{elec} is the fraction of spin components excited (g_{elec}=3). If we assume a cubic volume element and square pixels of size $\tilde{h}$, then $V = \tilde{h}^3/M^3$, where M is the magnification, and the sheet thickness, t, is $\tilde{h}/M$. Using the notation of Ref. [10], the quantity $V\eta_{coll}$ is equal to $\tilde{h}^3/M/[4f_{\#}(M+1)]^2$.

As an example, consider the case of a lean H_2/air flame at 1 atm. and 2300K, with the mole fraction of O_2, X_{O2}, equal to 2%. The quantity $NPP_{max}/V\eta_{coll}$ is calculated for several LIF transition options, and these are presented in Table 1. Also shown in Table 1 are required

Table 1: Calculated LIF Signal Maxima, per collection volume

Transition	Φ_{max} mJ/cm^2	$\frac{NPP_{max}}{V\eta_{coll}}$ cm^{-3}	$V\eta_{coll}$ for *NPP*=4000 cm^3
(7,1) P(17)	200	$4.9\cdot10^{10}$	$8.2\cdot10^{-8}$
(10,2) P(11)	5	$1.3\cdot10^{10}$	$3.1\cdot10^{-7}$
(15,3) $R_1(11)$	1	$3.8\cdot10^{9}$	$1.1\cdot10^{-6}$
(0,6) R(17)	100	$8.0\cdot10^{9}$	$5.0\cdot10^{-7}$
(2,7) P(9)	4	$7.3\cdot10^{8}$	$5.5\cdot10^{-6}$

values of $V\eta_{coll}$ to achieve *NPP*=4000. This value was chosen as it provides 400 photoelectrons per pixel (and a noise-to-signal ratio of 1/20, or 5%) for a combined filter and detector efficiency of 10%. In order to convert these values to signal levels, a collection geometry is required. Table 2 presents several representative values for the collection parameters, M, $f_{\#}$, and $\tilde{h}$, and the resulting $V\eta_{coll}$ and spatial resolution, t. In order to

Table 2: Typical Collection Parameters

M	$f_{\#}$	$\tilde{h}$, μm	$V\eta_{coll}$, cm^3	$t=\tilde{h}/M$, μm
2	1.4	50	$2.21\cdot10^{-10}$	25
2	1.4	200	$1.42\cdot10^{-8}$	100
1	2	50	$4.88\cdot10^{-10}$	50
1	2	200	$3.12\cdot10^{-8}$	200
0.5	4.5	50	$3.43\cdot10^{-10}$	100
0.5	4.5	200	$2.19\cdot10^{-8}$	400

achieve the different values of $\tilde{h}$, binning of pixels will probably be required. Note that, in order to offset the low levels of $NPP_{max}/V\eta_{coll}$, and allow for spectral filtering and detector quantum efficiency, both of which further degrade the signal, it is necessary to operate with $V\eta_{coll}$ on the order of 10^{-8} to 10^{-7} cm^3, even for the most efficient transitions. These levels of $V\eta_{coll}$ are achievable only with spatial resolution on the order of 200-400 μm. The less efficient transitions may require that spatial resolution be limited to near 1 mm. The result of this calculation indicates that, if O_2 S-R LIF is to be used, the spatial resolution will need to be limited, possibly severely, in order to remain in the non-depleting, linear signal regime.

Summary

A 3-level model has been developed to simulate the O_2 Schumann-Runge laser-induced fluorescence process. Calculations using the model compare favorably with available experimental data, and these calculations indicate that population depletion causes the signal in many cases to respond sublinearly to excitation laser fluence, even for low to moderate values of the fluence. The implication of this sublinear response is that, in order to remain in the linear regime, and hence in order to be able to relate the signal to lower state population, very low laser fluences are required. These low fluences, combined with the fact that predissociation of the O_2 *B*-state results in very low fluorescence yields, require that the spatial resolution in an O_2 Schumann-Runge LIF be severely limited. This model provides a guide for design of such an O_2 LIF experiment, and may be used to ascertain, a priori, whether the achievable spatial resolution is sufficient for resolution of the spatial scales of interest.

References

[1] Massey, G.A.; and Lemon, C.J.:"Feasibility of Measuring Temperature and Density Fluctuations in Air Using Laser-Induced O_2 Fluorescence," *IEEE Journal of Quantum Electronics*, **QE-20**(5), 454 (1984).

[2] Laufer, Gabriel; Robert L. McKenzie and Douglas G. Fletcher: "Method for measuring temperatures and densities in hypersonic wind tunnel air flows using laser-induced O_2 fluorescence," *Applied Optics*, **29**(33), 4873 (1990).

[3] Lee, Michael P.; Paul, Phillip H.; and Ronald K. Hanson, "Laser-fluorescence imaging of O_2 in combustion flows using an ArF laser," *Optics Letters*, **11**(1), 7 (1986).

[4] Goldsmith, J.E.M; and R.J.M.Anderson, "Laser-induced fluorescence spectroscopy and imaging of molecular oxygen in flames," *Optics Letters*, **11**(2), 67 (1986).

[5] Copeland, Richard A; et al., "Vibrationally excited O_2 in flames: Measurements on v"=9-11 by laser-induced fluorescence," *Journal of Chemical Physics*, **86**(5), 2500 (1987).

[6] Andresen, Peter; et al., "Laser-induced fluorescence with tunable excimer lasers as a possible method for instantaneous temperature field measurements at high pressures: checks with an atmospheric flame," *Applied Optics*, **27**(2), 365 (1988).

[7] Kim, G.-S.; et al., "Identification and Imaging of Hot O_2 (v"=2, 3, or 4) in Hydrogen Flames Using 193 nm- and 210 nm-range Light," *Applied Physics B*, **53**, 180 (1991).

[8] Grinstead, J.H.; Laufer, G.; and J.C. McDaniel, Jr.: "Single-pulse, two-line temperature-measurement technique using KrF laser-induced O_2 fluorescence," *Applied Optics*, **34**(24), 5501 (1995).

[9] Miles, R.; et al., "Velocity measurements by vibrational tagging and fluorescent probing of oxygen," *Optics Letters*, **12**(11) 861 (1987).

[10] Eckbreth, Alan C.: Laser Diagnostics for Combustion Temperature and Species, Energy and Engineering Science Series, **7**, A.K.Gupta and D. G. Lilley (eds.), Abacus Press, Cambridge, Mass., 1988.

[11] Octave, A high-level interactive language for numerical computations, Copyright © 1993, 1994, 1995 John W. Eaton; available via public ftp from bevo.che.wisc.edu/pub/octave.

[12] Radhakrishnan, Krishnan; and Alan C. Hindmarsh: "Description and Use of LSODE, the Livermore Solver for Ordinary Differential Equations," NASA Reference Publication 1327, 1993.

[13] Tatum, J.B.: "Hönl-London Factors for $^3\Sigma^{\pm}$-$^3\Sigma^{\pm}$ Transitions," *Canadian Journal of Physics*, **44**, 2944 (1966).

[14] Allison, A.C; Dalgarno, A.; and N.W.Pasachoff, "Absorption by Vibrationally Excited Molecular Oxygen in the Schumann-Runge Continuum," *Planet. Space Sci.*, **19**, 1463 (1971).

[15] Lewis, B.R.; Gibson, S.T; and P.M.Dooley, "Fine-Structure dependence of predissociation linewidth in the Schumann-Runge bands of molecular oxygen," *Journal of Chemical Physics*, **100**(10), 7012 (1994).

[16] Lewis, B.R.: personal communication.

[17] Smith, Earl W.: "Absorption and dispersion in the O_2 microwave spectrum at atmospheric pressures," *Journal of Chemical Physics*, **74**(12), 6658 (1981).

[18] Diskin, Glenn S.; Lempert, Walter R.; and Richard B. Miles:

"Observation of Vibrational Relaxation Dynamics in $X^3\Sigma_g^-$ Oxygen following Stimulated Raman Excitation to the v=1 Level: Implications for the RELIEF Flow Tagging Technique," AIAA paper 96-0301, presented at the 34th Aerospace Sciences Meeting and Exhibit, Reno, Nevada, January, 1996.

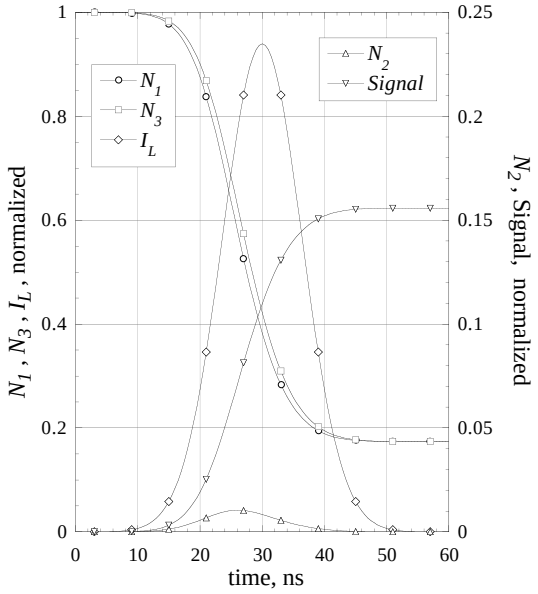

Figure 1. Calculated time histories for (15,3) $R_1(11)$ transition. Φ = 25 mJ/cm^2; Trot = 300K; p = 1 atm.

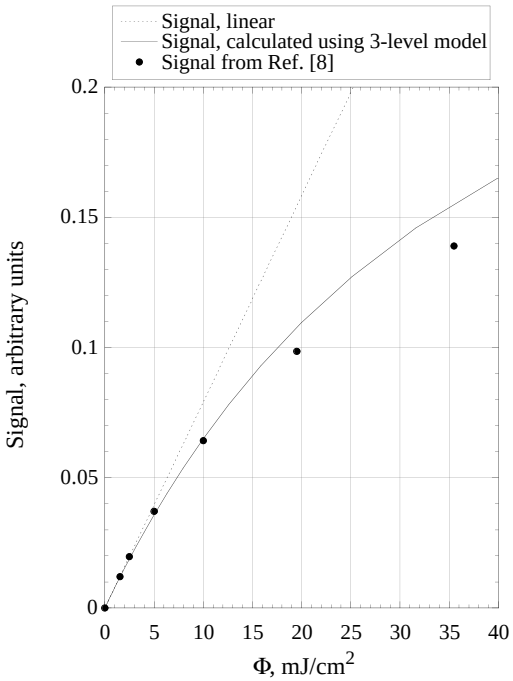

Figure 2(a). Variation of LIF Signal with laser fluence, Φ, for (2,7) P(9) transition at 1800K, 1 atm.

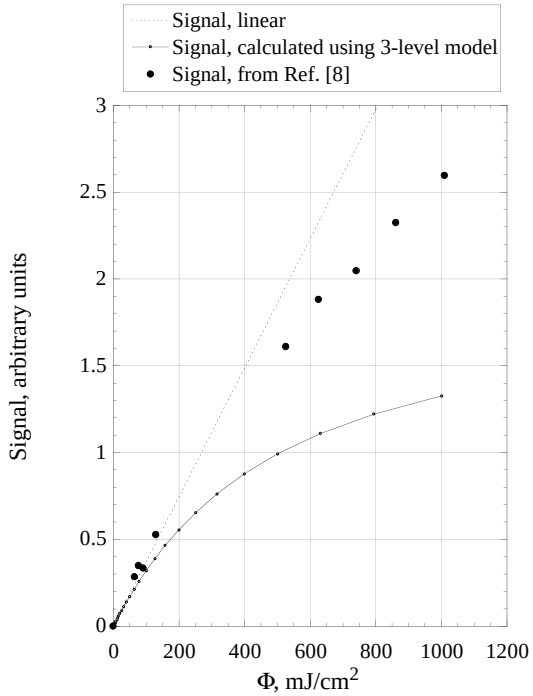

Figure 2(b). Variation of LIF Signal with laser fluence, Φ, for (0,6) R(17) transition at 1800K, 1 atm.

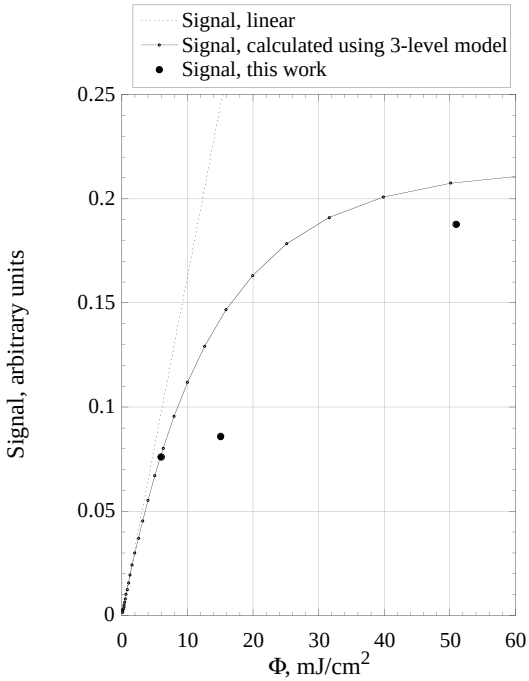

Figure 3. Variation of LIF Signal with laser fluence, Φ, for (15,3) $R_1(11)$ transition at 300K, 1 atm.